

Image Inpainting for High-Resolution Textures using CNN Texture Synthesis

Pascal Laube, Michael Grunwald, Matthias O. Franz & Georg Umlauf
 Institute for Optical Systems, University of Applied Sciences Constance, Germany
 plaube@htwg-konstanz.de

Abstract

Deep neural networks have been successfully applied to problems such as image segmentation, image super-resolution, coloration and image inpainting. In this work we propose the use of convolutional neural networks (CNN) for image inpainting of large regions in high-resolution textures. Due to limited computational resources processing high-resolution images with neural networks is still an open problem. Existing methods separate inpainting of global structure and the transfer of details, which leads to blurry results and loss of global coherence in the detail transfer step. Based on advances in texture synthesis using CNNs we propose patch-based image inpainting by a single network topology that is able to optimize for global as well as detail texture statistics. Our method is capable of filling large inpainting regions, oftentimes exceeding quality of comparable methods for images of high-resolution (2048x2048px). For reference patch look-up we propose to use the same summary statistics that are used in the inpainting process.

1. Introduction

Image inpainting is the process of filling missing or corrupted regions in images based on surrounding image information so that the result looks visually plausible. Recently machine learning techniques have been applied successfully to the problem of inpainting. In [15] Pathak et al. have shown that so called context-encoders are able to fill missing regions in natural images. While being able to propagate global structure the results lack details and are blurry. Because of this Yang et al. [21] propose a second network for detail transfer to the inpainting region after the content inpainting step. While this helps to compensate blurriness, it is not removed, and transitions in-between detail application patches are clearly visible. This approach is still limited to lower resolution because of content inpainting and loses some of the global structure in the detail transfer process which renders it unsuitable for high-resolution textures. To resolve these issues we propose an inpainting approach that produces results that satisfy global structure

and contain blurry-free details. We fill the inpainting region by synthesis of new texture patch by patch, which enables us to process high-resolution textures. Our inpainting approach provides smooth transition between the sampling and the inpainting region as well as in-between patches. We propose a single CNN topology that is able to shift focus from optimizing detail to global statistics and vice versa. Since we solely focus on textures we apply texture statistics for synthesis that are able to capture important aspects of material perception in humans. For reference patch look-up we propose to use the same statistics that are used in patch synthesis. Sections of this paper are arranged as follows. We will first give an overview over related works in Sec. 2. The process of texture synthesis by CNNs is then explained in Sec. 3. In Sec. 4 we present our inpainting approach, followed by results in Sec. 5 and discussion in Sec. 6. We conclude in Sec. 7.

2. Related works

Most image inpainting approaches are based on sampling existing information surrounding the inpainting region, which is called exemplar-based [2, 4, 6, 7, 11, 12, 20] inpainting. Many exemplar-based methods approach inpainting in a copy-paste fashion. A very well known method is the work by Criminisi et al. [4] which applies this methodology but restricts the fill order to propagate linear structures (isophotes) first. This process has been further improved by Barnes et al. [2] who contribute a fast way for randomized correspondence search to find suitable patches. These approaches are very dependent on patch-size and fail to satisfy global statistics that are not captured within a single patch. This is a problem since texture is defined as the repetition of simpler elements together with some stochasticity of global repetitions as well as local sub-patterns. Recently deep learning approaches have been applied successfully to the problems of texture synthesis and image inpainting [5, 9, 10, 13]. First introduced by Gatys et al. in [8] texture synthesis by CNNs has shown to surpass well known methods like [16] for many different examples. Wallis et al. [19] recently showed that artificial images produced from a parametric texture model closely match texture appearance for

humans. Especially, the CNN texture model of [8] and the extension by Liu [14] are able to capture important aspects of material perception in humans. For many textures the synthesis results are indistinguishable under foveal inspection. Other methods like the already mentioned methods by Phatak et al. [15] and Yang et al. [21] train auto-encoder like networks called context-encoders for inpainting. They use a combination of classic pixel-wise reconstruction loss as well as an adversarial loss term and a detail transfer network.

3. Texture synthesis

Since our inpainting approach strongly relies on the method introduced by Gatys et al. [8] we will adapt the same notation. In this approach new texture is synthesized by CNN input optimization. Like [8] we use a VGG-19 [17] analysis network pre-trained on the image-net data set to compute a spatial summary statistic, the Gramian, of some vectorized texture \mathbf{x} of size P . By then optimizing an initialization vector $\hat{\mathbf{x}}$ with a second VGG-19 synthesis network to satisfy the summary statistics of the analysis network new texture can be synthesized. The Gramian of some network Layer l is defined as

$$\mathbf{G}_{ij}^l = \sum_k \mathbf{F}_{ik}^l \mathbf{F}_{jk}^l, \quad (1)$$

where \mathbf{F}_{ik}^l is feature map i and \mathbf{F}_{jk}^l feature map j at location k given input \mathbf{x} . These inner products of filter activations of different layers are then used to define a synthesis loss

$$\mathcal{L}_s(\mathbf{x}, \hat{\mathbf{x}}) = \sum_{l=0}^L \frac{1}{2N_l^2 M_l^2} \sum_{i,j} (\mathbf{G}_{ij}^l - \hat{\mathbf{G}}_{ij}^l)^2,$$

with N_l feature maps of size M_l at layer l . Since this can be seen as an averaging over feature map positions global texture coherence is lost. Berger and Memisevic [3] introduce a second cross-correlation loss by computing Gramians between feature maps \mathbf{F}^l and a spatial translation T of the filter maps $T(\mathbf{F}^l)$. By discarding either rows or columns of feature maps one can now compute correlations of features at some location $k = (x, y)$ and a shifted location $T_{x,+\delta}(k) = (x + \delta, y)$ or $T_{y,+\delta}(k) = (x, y + \delta)$. The horizontally translated Gramian becomes

$$\mathbf{G}_{x,\delta,ij}^l = \sum_k T_{x,+\delta}(\mathbf{F}_{ik}^l) T_{x,-\delta}(\mathbf{F}_{jk}^l), \quad (2)$$

and $\mathbf{G}_{y,\delta,ij}^l$ analogous. The cross-correlation loss \mathcal{L}_{cc} for an arbitrary shift δ is defined as

$$\mathcal{L}_{cc}(\mathbf{x}, \hat{\mathbf{x}}) = \sum_{l,i,j} \frac{(\mathbf{G}_{x,\delta,ij}^l - \hat{\mathbf{G}}_{x,\delta,ij}^l)^2 + (\mathbf{G}_{y,\delta,ij}^l - \hat{\mathbf{G}}_{y,\delta,ij}^l)^2}{4N_l^2 M_l^2}.$$

The combined loss is then defined as

$$\mathcal{L}_{s,cc}(\mathbf{x}, \hat{\mathbf{x}}) = w_s \mathcal{L}_s + w_{cc} \mathcal{L}_{cc},$$

with weight factors w_s and w_{cc} .

4. Patch-based texture synthesis for image inpainting

In this section we will present our novel approach for patch-based inpainting of high-resolution textures using CNN texture synthesis.

4.1. Patch-based texture synthesis

Given some image Θ with high-resolution texture Φ we propose the application of the synthesis method introduced in Sec. 3 on different scales of resolution. We use a single neural network topology to fill inpainting region Ω . The approach is explained in conjunction with the sample texture in Fig. 1.

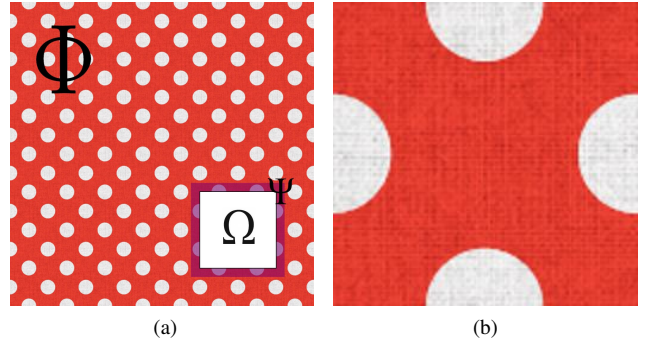


Figure 1: (a) Image Θ (2048x2048px) with inpainting region Ω , boundary Ψ and Dots cloth texture Φ . (b) Closeup on a region of 1a (256x256px).

A schematic overview of our setup is given in Fig. 2. For inpainting of region Ω one needs to satisfy global statistics (dots pattern) as well as the detail statistics (cloth pattern). We propose to inpaint region Ω patch by patch (or sliding-window) with each patch satisfying global as well as detail statistics. Our inpainting network consists of two main branches: The *global branch* with focus on optimization for global statistics and the *detail branch* to satisfy detail statistics. Each branch consists of a VGG-19 network pre-trained on the ImageNet data set. We further define the input to the *detail branch* as $\hat{\mathbf{x}}_d$, and to the *global branch* as $\hat{\mathbf{x}}_g$. While $\hat{\mathbf{x}}_d$ is the actual patch optimizing Ω in native resolution, $\hat{\mathbf{x}}_g$ is initialized with a Q -times average-pooled cutout of Θ so that this cutout fully contains Ω and boundary Ψ . Before a shift of $\hat{\mathbf{x}}_d$ to a new location we update Ω with the synthesis result in $\hat{\mathbf{x}}_d$ and reinitialize $\hat{\mathbf{x}}_g$. Only $\hat{\mathbf{x}}_d$ is optimized in the synthesis process. An interconnection of

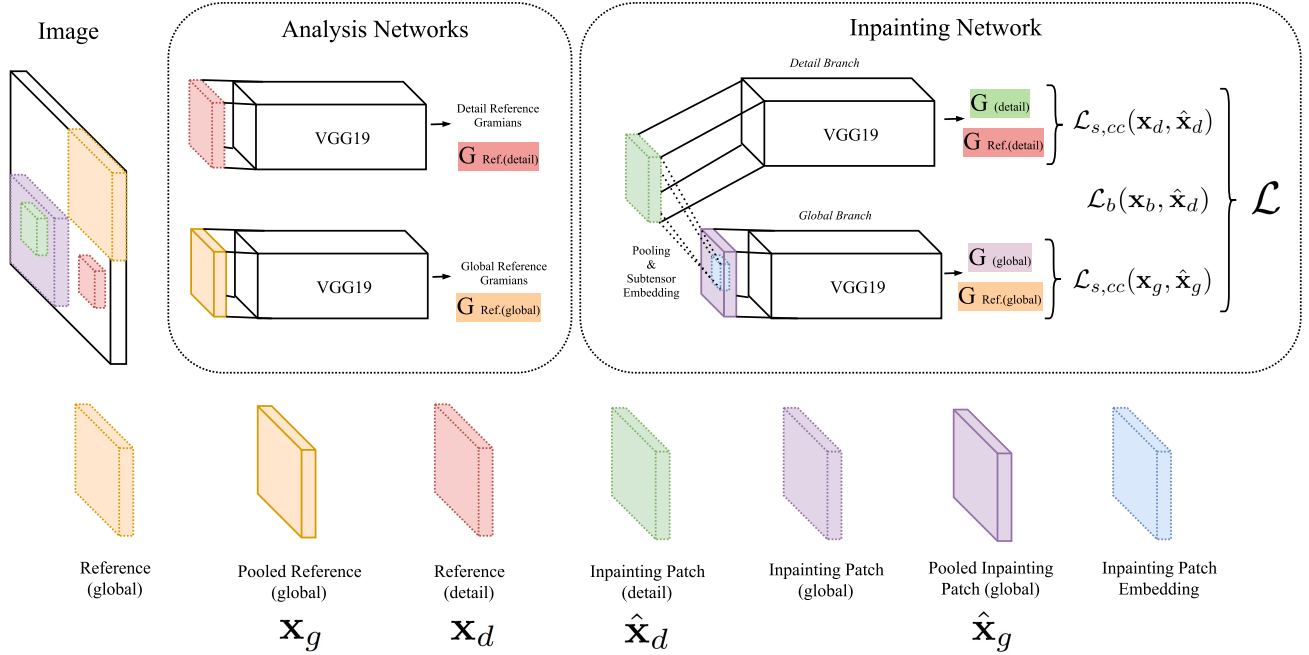


Figure 2: Network topology

the two branches is achieved by embedding $\hat{\mathbf{x}}_d$ into $\hat{\mathbf{x}}_g$. We introduce Q average-pooling-layers in-between $\hat{\mathbf{x}}_d$ and $\hat{\mathbf{x}}_g$ before the embedding. Pooled $\hat{\mathbf{x}}_d$ is then embedded at the correct (pooled) position in $\hat{\mathbf{x}}_g$ so that it becomes a subtensor. Depending on the size of Ω , Q needs to be adjusted as a parameter before inpainting. As a result network topology needs to change. Since this change does not introduce new weights it is easily adaptable without training for different sizes of Ω or different resolutions.

For synthesis as described in Sec. 3 suitable reference textures \mathbf{x}_d and \mathbf{x}_g are needed as input for the analysis networks. We will describe reference patch look-up in Sec. 4.2. While \mathbf{x}_g needs to be initialized only once at the beginning of the inpainting process, \mathbf{x}_d is reinitialized with a new reference for every new position of the inpainting patch $\hat{\mathbf{x}}_d$. We further define a boundary loss, that limits the optimization of region Ψ inside $\hat{\mathbf{x}}_d$ in the input domain. We define the boundary loss as

$$\mathcal{L}_b(\mathbf{x}, \hat{\mathbf{x}}) = \frac{1}{P} \sum (\mathbf{m}\mathbf{x} - \mathbf{m}\hat{\mathbf{x}})^2, \quad (3)$$

where the binary mask \mathbf{m} equals 0, if $\mathbf{m}_i \in \Omega$, and 1 otherwise. The combined loss over both branches together with boundary loss becomes

$$\mathcal{L} = w_d \mathcal{L}_{s,cc}(\mathbf{x}_d, \hat{\mathbf{x}}_d) + w_g \mathcal{L}_{s,cc}(\mathbf{x}_g, \hat{\mathbf{x}}_g) + w_b \mathcal{L}_b(\mathbf{x}_b, \hat{\mathbf{x}}_d),$$

where w_d , w_g , and w_b are weight terms. \mathbf{x}_b is initialized with $\hat{\mathbf{x}}_d$ before optimization and does change for each new position of $\hat{\mathbf{x}}_d$.

4.2. Patch distance by Gramians

For synthesis of patch $\hat{\mathbf{x}}_d$ suitable reference patches \mathbf{x}_d , and \mathbf{x}_g are needed. Initial $\hat{\mathbf{x}}_d$ is a cutout of Θ containing parts of Ψ as well as parts of Ω while $\hat{\mathbf{x}}_g$ completely contains Ψ and Ω . One now has to find closest patches from Φ matching Ψ inside $\hat{\mathbf{x}}_d$, and $\hat{\mathbf{x}}_g$ as candidates for \mathbf{x}_d , and \mathbf{x}_g . Instead of MSE we propose to use the distance of texture Gramians as a similarity measure. Values inside inpainting region Ω are unknown. Because of this we propose masking Ω for each individual feature map to remove Ω related correlations from any of the resulting Gramians. Since network input up to some layer l has passed through pooling as well as convolutional layers we need to adapt feature map masks to compensate for these operations. In a first step the initial binary mask \mathbf{m} from Eq. (3), needs to be adapted in size to account for pooling layers. This is done by applying each max-pooling step of VGG-19 that has been applied up to layer l to the mask \mathbf{m}^l which is responsible for masking feature maps \mathbf{F}^l . In a second step one needs to account for the propagation of Ω into Ψ by convolutions. Since convolutional filters of VGG-19 are of size 3x3, inpainting region Ω propagates into Ψ one pixel at a time for each convolutional layer (comparable to binary-erosion). Simply discarding those pixels by setting them to zero in \mathbf{m}^l for each convolutional layer is too restrictive and would lead to masks with all values zero in late layers. Because of this we expand Ω by a smaller individual number of pixels e^l for each layer (see Sec. 5). In our experiments this expansion has proven to be sufficient for compensation.

Taking these considerations into account we define patch distance as

$$\Delta_G(\mathbf{x}, \hat{\mathbf{x}}) = \sum_{l,i,j} \left(\sum_k \mathbf{m}^l \mathbf{F}_{ik}^l \mathbf{F}_{jk}^l - \sum_k \mathbf{m}^l \hat{\mathbf{F}}_{ik}^l \hat{\mathbf{F}}_{jk}^l \right)^2.$$

4.3. Inpainting

For inpainting we propose a *two stage* inpainting process. At each stage $\hat{\mathbf{x}}_d$ is optimized by applying L-BFGS-B [22]. We initialize each color channel in region Ω with the corresponding color channel mean from Φ (see Fig. 3a). In the first stage we optimize focusing on the *global branch* by setting $w_d = 0$, $w_g = 1$. This leads to $\hat{\mathbf{x}}_d$ satisfying global statistics but at low resolution. Pooling larger input regions introduces color artifacts since loss is shared among pooled pixels as can be seen in Fig. 3b. We eliminate these color artifacts by converting Ω to greyscale (see Fig. 3c) with RGB weights $r = 0.212$, $g = 0.7154$, $b = 0.0721$. Only this structure is used for initialization of the second stage. In the second stage we set $w_d = 1$ and w_g to a value in the range of $[0.01, 0.1]$. This ensures focus on the optimization for detail statistics through the *detail branch* while constraining the optimization to also maintain global texture statistics.

One important consideration in classic patch-based inpainting is the order in which to fill Ω . For our approach this order is not important as long as the first patch overlaps with Ψ . We also make sure that consecutive patches overlap. Overlapping a patch by $\frac{1}{4}$ of its own size with surrounding texture has proven to be sufficient. To ensure a smooth transition in-between patches we apply image quilting [6] in overlapping regions. We chose to fill Ω in a top to bottom, left to right fashion (see Fig. 3d). As a results of our experiments we set $w_s = 1e6$ and $w_{cc} = 1e7$ for inpainting of 8-bit color images. Choosing w_b in the range $[10, 50]$ has shown to be sufficient. The large difference between Gramian-based loss weights and weights related to loss in pixel space results from different value ranges.

5. Results

We present inpainting results of exemplar high resolution textures. All textures have a resolution of 2048x2048px while the inpainting region Ω is of size 512x512px. For initialization of synthesis as well as analysis networks we used parameters of a pre-trained VGG-19 network provided by [8] and transferred these parameters to our own theano-based [18] implementation. The network input size (inpainting patch size) for all networks is 256x256px. For definition of \mathcal{L} we use Gramians of layers *conv1_1*, *pool1*, *pool2*, *pool3* and *pool4* leading to $L = 5$. For patch distance computation we define pixel expansions $\mathbf{e} = (1, 1, 2, 3, 2)$, and for shift δ of translated Gramians $\mathbf{G}_{x,\delta}^l$ and $\mathbf{G}_{y,\delta}^l$ we define $\delta = (6, 6, 5, 4, 3)$. For our examples $Q = 2$ pooling layers suffices to ensure that Ω as well as Ψ fits into $\hat{\mathbf{x}}_g$.

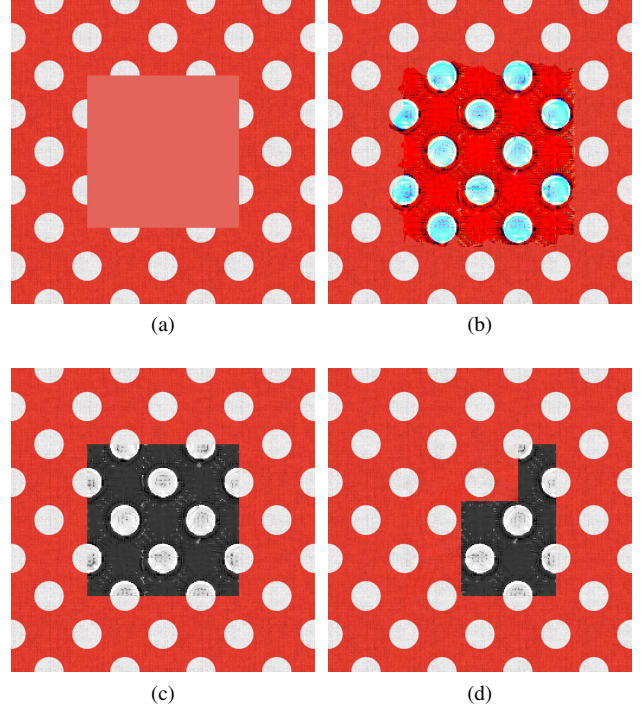


Figure 3: (a) Initialization with image mean. (b) Stage one inpainting with $w_d = 0$, $w_g = 1$. (c) Greyscale initialization of stage two. (d) Optimization for texture detail.

To find suitable reference patches \mathbf{x}_d and \mathbf{x}_g region Φ is searched at a step size of 64px. Since we are not dependent on exact matches in terms of MSE this step size is sufficient and speeds up reference patch look-up. Inpainting of the exemplar textures was done using a Nvidia GeForce 1080 Ti and took roughly 8 min strongly depending on the number of iterations of the L-BFGS-B [22] optimization.

We compare our approach for patch-based inpainting by texture synthesis (PITS) to the exemplar-based method of Criminisi et al. [4] (EBI) as well as the Content-Aware Fill method of Photoshop CS7 (PSCS7) which is a combination of methods [2] and [20]. We do not compare to method [21] since we found no suitable set of parameters that yielded acceptable results for inpainting high-resolution textures larger 512x512px. We compare results for each example on the basis of MSE and structural dissimilarity measure (DSSIM) [1] of original texture and inpainted Ω in Table 1. We also present a visual evaluation in Fig. 8. For the first exemplar texture *Dots* (Fig. 5a) we arrive at smaller values for DSSIM and MSE as well as a better visual quality. While EBI fails to inpaint Ω reasonably the result by PSCS7 looks visually coherent but fails to reconstruct dots as perfect circles. PITS manages to produce visually appealing structure globally as well as locally. For the *Bricks* example in Fig. 5b PITS again arrives at smallest DSSIM

while having a slightly larger MSE than EBI. Here MSE is not well suited as a quality measure since it is clearly visible that EBI again fails to provide a visually plausible result. In terms of structural continuity PITS produces better looking results than PSCS7. When drastically enlarged one can see that for the *Bricks* example our method can lead to some slight change of color within bricks which is a result of the color variety in-between reference patches. For the *Wood* texture PITS arrives at a slightly larger DSSIM than EBI. Visually PITS inpaints Ω reasonably while EBI creates a visually unconvincing result. While PSCS7 arrives at smaller values for MSE as well as DSSIM similar knotholes in Ω directly copied over from Φ can be spotted.

Error	PITS	EBI	PSCS7
<i>Dots</i>			
DSSIM	0.057	0.191	0.064
MSE	179.9	7387.4	891.1
<i>Bricks</i>			
DSSIM	0.284	0.294	0.302
MSE	1090.6	1034.2	1120.8
<i>Wood</i>			
DSSIM	0.081	0.077	0.057
MSE	271.1	531.3	162.7

Table 1: Comparison of inpainting results of methods PITS, EBI and PSCS7 on textures Dots, Bricks, and Wood by DSSIM and MSE.

6. Discussion

As presented in Sec. 5 our method is able to inpaint high-resolution texture satisfying global structure as well as details. While surpassing other methods in terms of maintaining texture statistics results may contain color deviations in-between inpainted patches depending strongly on reference patch selection. This especially is the case when the source region Φ has a very diverse color palette like the example in Fig. 5b. Using the difference of masked Gramians as a metric for patch distance has major benefits for our inpainting approach over using simple MSE. Since we are not dependent on reference textures \mathbf{x}_d or \mathbf{x}_g exactly matching Ψ inside $\hat{\mathbf{x}}_d$ or $\hat{\mathbf{x}}_g$ in terms of MSE, we can reduce the number of samples taken from Φ in reference patch look-up. MSE is not well suited as a measure of texture similarity as can be seen from the result of EBI for inpainting the *Bricks* example texture. While achieving the lowest value for MSE, the approach fails when examined visually. Due to the averaging of feature information inside Gramians, global spatial information is lost. This enables the Gramian to represent texture invariant to rotation and translation to some degree (see Fig. 4). Because our loss term \mathcal{L} is based on the difference of Gramians this further ensures that Ψ inside $\hat{\mathbf{x}}$ already satisfies target statistics to some extent.

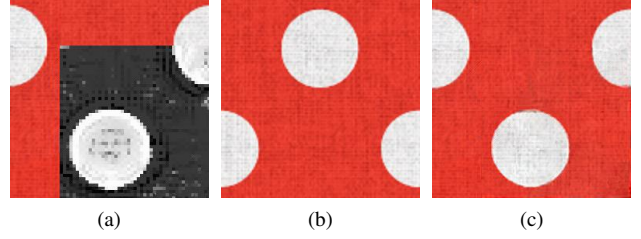


Figure 4: (a) Inpainting patch $\hat{\mathbf{x}}_d$. (b) Closest reference patch from Φ . (c) Inpainting result.

Major strength of our method is the correct inpainting of global structure while also maintaining details. When choosing w_d and w_g one needs to be aware of the trade-off introduced. While higher w_g ensures persistence of global statistics it also introduces artifacts as a result of pooling $\hat{\mathbf{x}}_d$ before subtensor embedding and vice versa. Higher w_d lays larger emphasis on details while possibly violating global structure. This trade-off is further influenced by the number of poolings Q .

7. Conclusion

We present a patch-based approach for image inpainting of high resolution textures using CNN texture synthesis. Our method is capable of filling large inpainting regions that are visually coherent in global structure as well as details. We also introduce a distance metric for the comparison of patches based on summary statistics by using masked Gramians. For future work we plan to develop our method further for inpainting of natural scenes. We would also like to apply this concept to 3D surface reconstruction.

Acknowledgments

This research is funded by the Federal Ministry of Education and Research (BMBF) of Germany (project number 02P14A035).

References

- [1] F. E. Al-Obaidi. Image quality assessment for defocused blur images. *American Journal of Signal Processing*, 5(3):51–55, 2015.
- [2] C. Barnes, E. Shechtman, A. Finkelstein, and D. B. Goldman. Patchmatch: A randomized correspondence algorithm for structural image editing. *ACM Trans. Graph.*, 28(3):24–1, 2009.
- [3] G. Berger and R. Memisevic. Incorporating long-range consistency in cnn-based texture generation. *arXiv preprint arXiv:1606.01286*, 2016.
- [4] A. Criminisi, P. Pérez, and K. Toyama. Region filling and object removal by exemplar-based image inpainting. *IEEE Transactions on image processing*, 13(9):1200–1212, 2004.

- [5] A. Dosovitskiy and T. Brox. Generating images with perceptual similarity metrics based on deep networks. In *Advances in Neural Information Processing Systems*, pages 658–666, 2016.
- [6] A. A. Efros and W. T. Freeman. Image quilting for texture synthesis and transfer. In *Proceedings of the 28th annual conference on Computer graphics and interactive techniques*, pages 341–346. ACM, 2001.
- [7] A. A. Efros and T. K. Leung. Texture synthesis by non-parametric sampling. In *Computer Vision, 1999. The Proceedings of the Seventh IEEE International Conference on*, volume 2, pages 1033–1038. IEEE, 1999.
- [8] L. Gatys, A. S. Ecker, and M. Bethge. Texture synthesis using convolutional neural networks. In *Advances in Neural Information Processing Systems*, pages 262–270, 2015.
- [9] L. A. Gatys, A. S. Ecker, and M. Bethge. Image style transfer using convolutional neural networks. In *Proceedings of the IEEE Conference on Computer Vision and Pattern Recognition*, pages 2414–2423, 2016.
- [10] J. Johnson, A. Alahi, and L. Fei-Fei. Perceptual losses for real-time style transfer and super-resolution. In *European Conference on Computer Vision*, pages 694–711. Springer, 2016.
- [11] V. Kwatra, I. Essa, A. Bobick, and N. Kwatra. Texture optimization for example-based synthesis. *ACM Transactions on Graphics (ToG)*, 24(3):795–802, 2005.
- [12] V. Kwatra, A. Schödl, I. Essa, G. Turk, and A. Bobick. Graphcut textures: image and video synthesis using graph cuts. In *ACM Transactions on Graphics (ToG)*, volume 22, pages 277–286. ACM, 2003.
- [13] C. Li and M. Wand. Combining markov random fields and convolutional neural networks for image synthesis. In *Proceedings of the IEEE Conference on Computer Vision and Pattern Recognition*, pages 2479–2486, 2016.
- [14] G. Liu, Y. Gousseau, and G.-S. Xia. Texture synthesis through convolutional neural networks and spectrum constraints. In *Pattern Recognition (ICPR), 2016 23rd International Conference on*, pages 3234–3239. IEEE, 2016.
- [15] D. Pathak, P. Krahenbuhl, J. Donahue, T. Darrell, and A. A. Efros. Context encoders: Feature learning by inpainting. In *Proceedings of the IEEE Conference on Computer Vision and Pattern Recognition*, pages 2536–2544, 2016.
- [16] J. Portilla and E. P. Simoncelli. A parametric texture model based on joint statistics of complex wavelet coefficients. *International journal of computer vision*, 40(1):49–70, 2000.
- [17] K. Simonyan and A. Zisserman. Very deep convolutional networks for large-scale image recognition. *arXiv preprint arXiv:1409.1556*, 2014.
- [18] Theano Development Team. Theano: A Python framework for fast computation of mathematical expressions. *arXiv e-prints*, abs/1605.02688, May 2016.
- [19] T. S. Wallis, C. M. Funke, A. S. Ecker, L. A. Gatys, F. A. Wichmann, and M. Bethge. A parametric texture model based on deep convolutional features closely matches texture appearance for humans. *Journal of Vision*, 17(12):5–5, 2017.
- [20] Y. Wexler, E. Shechtman, and M. Irani. Space-time completion of video. *IEEE Transactions on pattern analysis and machine intelligence*, 29(3), 2007.
- [21] C. Yang, X. Lu, Z. Lin, E. Shechtman, O. Wang, and H. Li. High-resolution image inpainting using multi-scale neural patch synthesis. *arXiv preprint arXiv:1611.09969*, 2016.
- [22] C. Zhu, R. H. Byrd, P. Lu, and J. Nocedal. Algorithm 778: L-bfgs-b: Fortran subroutines for large-scale bound-constrained optimization. *ACM Transactions on Mathematical Software (TOMS)*, 23(4):550–560, 1997.

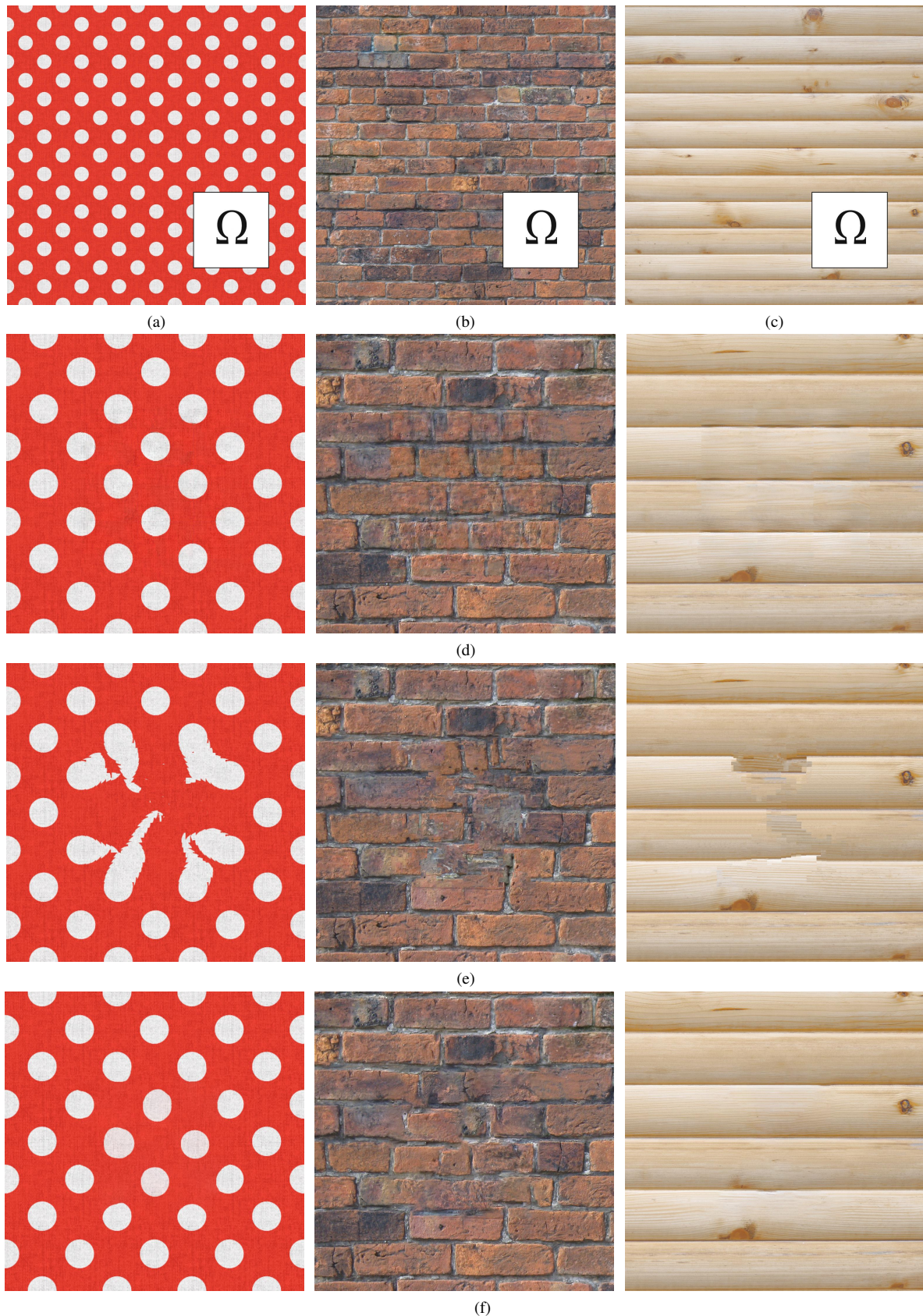


Figure 5: (a)-(c) Original with inpainting region Ω . Close-up on inpainting results of (d) PITs, (e) EBI, and (f) PSCS7.

Supplementary Material

Further inpainting results (2048x2048) of our approach: (a) Original with inpainting region Ω (512x512), (b) result of inpainting global structure (stage one), (c) final inpainting result, (d) close-up of the inpainted region.

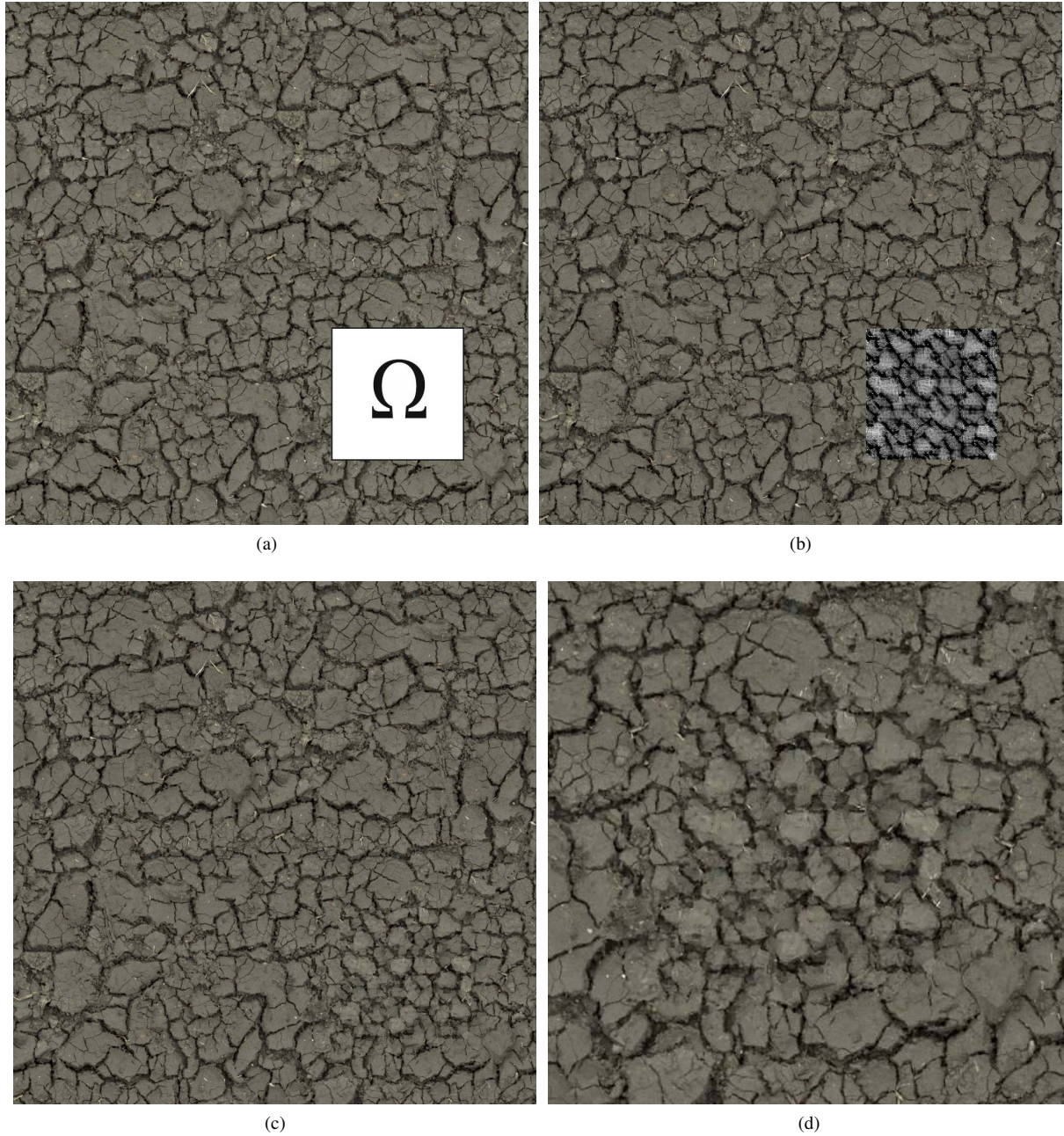
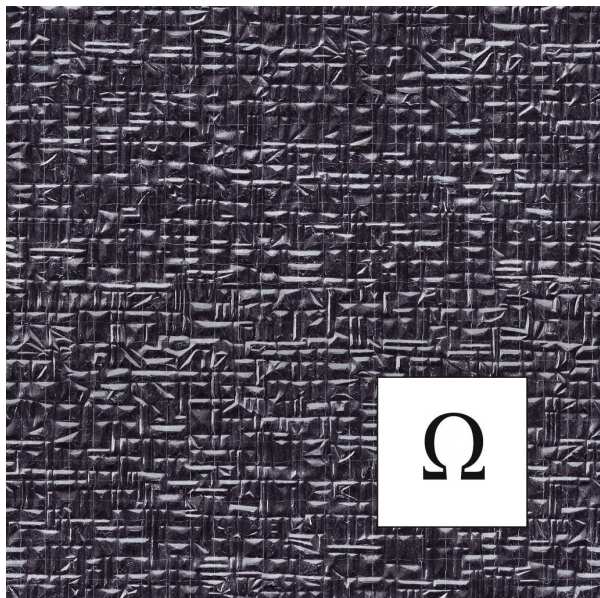
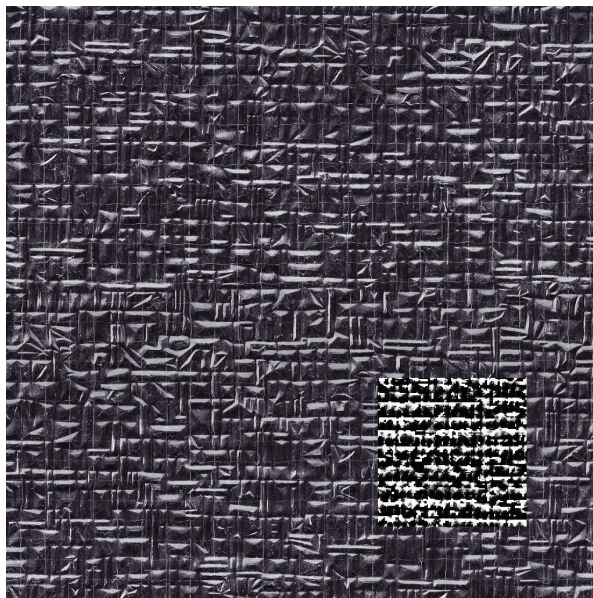


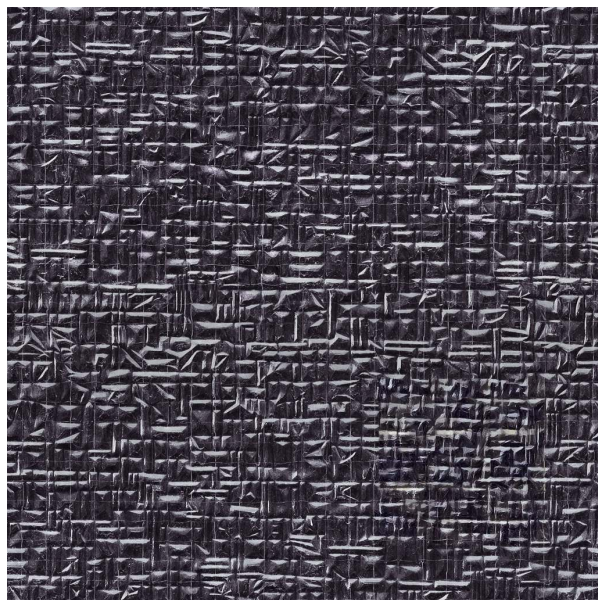
Figure 6



(a)



(b)



(c)



(d)

Figure 7



(a)



(b)



(c)



(d)

Figure 8